Electrochemical quartz crystal microbalance measurements of CO adsorption and oxidation on Pt in various electrolytes

Please check the document version of this publication:

• A submitted manuscript is the version of the article upon submission and before peer-review. There can be important differences between the submitted version and the official published version of record. People interested in the research are advised to contact the author for the final version of the publication, or visit the DOI to the publisher's website.
• The final author version and the galley proof are versions of the publication after peer review.
• The final published version features the final layout of the paper including the volume, issue and page numbers.

Link to publication

Electrochemical quartz crystal microbalance measurements of CO adsorption and oxidation on Pt in various electrolytes

W. Visscher,* J. F. E. Gootzen, A. P. Cox and J. A. R. van Veen

Laboratory of Inorganic Chemistry and Catalysis, Eindhoven University of Technology, P.O. Box 513, 5600 MB Eindhoven, The Netherlands

Abstract—The adsorption behaviour of Pt was investigated with the electrochemical quartz microbalance during potential scanning in acid electrolytes. From the mass increase with potential it is concluded that in the potential range of hydrogen desorption and double layer both water and anions are adsorbed in H_2SO_4 and H_3PO_4, whereas in $HClO_4$ there is only adsorption of water molecules. The mass changes in the oxygen region indicate that anions are included in the oxide layer. The Pt/CO_{ads} system was studied in H_2SO_4, $HClO_4$ and H_3PO_4. The presence of adsorbed CO is observed as a mass increase with respect to the CO-free system. The results show that water is adsorbed on top of the adsorbed CO layer at low potentials. Moreover, it can be concluded from the mass-balance data that water molecules are attached to the hydrogen monolayer at 0.03 V vs R.H.E. in sulfuric and perchloric acid, but not in phosphoric acid. © 1997 Elsevier Science Ltd

Key words: electrochemical quartz crystal microbalance, Pt, water adsorption, anion adsorption, carbon monoxide

INTRODUCTION

The electrochemical quartz crystal microbalance (EQCM) is a very sensitive device for *in situ* monitoring of adsorption processes at electrodes, enabling detection of species even in submonolayer quantities [1–4].

The technique is based on the measurement of changes in the resonant frequency of a quartz crystal. By coating the crystal with metal, the system becomes an electrochemical mass sensor, capable of measuring mass changes of all species that ara attached to the electrode surface, including non-electrochemically active species such as electrolyte ions and water molecules. In a recent review on electrosorption studies, however, Horanyi [5] raises doubts whether water can indeed be measured with the EQCM.

For mass changes smaller than 0.5% of the total weight of the crystal, a linear correlation exists between the mass change (Δm) and the frequency change (Δf):

---

*Corresponding author.

$$\Delta m = -SA\Delta f \quad S = \frac{\sqrt{\rho_q \mu_q}}{2f_0^2},$$

where S = Sauerbrey constant which can be calculated from the quartz material constants; f_0 = resonant frequency; A = active area of the crystal; μ_q and ρ_q are shear modulus and density of quartz. $S = 17.67$ ng Hz^{-1} cm^{-2} for a crystal with resonant frequency of 5 MHz. The frequency change of the crystal in contact with a liquid with density (ρ_L) and viscosity (η_L) is also affected by viscosity change $\Delta(\sqrt{\rho_L \eta_L})$ in the interface:

$$\Delta f = -\frac{2f_0^2}{\sqrt{\rho_q \mu_q}} \left(\frac{\Delta m}{A} + \frac{\Delta\sqrt{\eta_L \rho_L}}{\sqrt{4\pi f_0}} \right).$$

Changes in the viscosity of the outer Helmholtz layer have been considered to interpret frequency changes that were measured in the double layer region on Au [6]. The roughness of the electrode can also play a role: liquid, trapped in surface cavities, will give an extra mass contribution. Moreover changes in the surface roughness can distort the results [7].

The mass balance results published up to now for the electrochemically well known system of Pt are contradicting. In sulfuric acid generally a mass increase during potential scanning from low to high values has been found, which was interpreted as an increase of water adsorption and/or anion adsorption [8–11].

For the electrochemically very similar system of Pt in perchloric acid both a mass increase and a mass decrease have been reported in the low potential range [12–14].

We wanted to apply the EQCM method for a further investigation of CO adsorbed on Pt, in particular, to find out whether water is co-adsorbed with CO. With ellipsometry an adsorbed CO layer was clearly observed [15], but its composition could not be established. For proper evaluation of the PtCO$_{ads}$ system detailed knowledge of the adsorption behaviour of Pt itself is required. So in this paper we will study: (i) the mass changes on Pt in the presence of different anions and (ii) the oxidation of adsorbed CO in different electrolytes.

EXPERIMENTAL

The electrochemical quartz crystal microbalance (Eco Chemie) is a (Teflon) probe which can be placed in an electrolyte solution, such that one side of the disc-shaped metal coated quartz crystal (area 0.374 cm^2) is in contact with the electrolyte. The frequency changes were measured with a Philips PM 6680B/016 frequency counter, the noise level is *ca* 0.5 Hz. The fundamental frequency of the quartz crystal (AT cut, Au coated) is 5 MHz and was obtained from Phelps Electronics.

For the electrochemical experiments the probe is connected with Autolab potentioscan PGSTAT 10 or 20; the frequency–potential changes can be recorded simultaneously with the voltammogram. All chemicals are p.a. grade solutions and were prepared with ultrapure water (Ecostat 18.2 MΩ); CO gas (Hoek Loos) purity is 4.7. The counterelectrode was a Pt foil; the reference electrode was a Hg/Hg$_2$SO$_4$, saturated K$_2$SO$_4$ reference electrode in acid electrolytes and a Hg/HgO in alkaline electrolyte. All potentials are referred to R.H.E.

Before the experiments argon was passed through to remove dissolved oxygen. All measurements were performed at Pt which was electrodeposited onto Au from 0.02 M (NH$_4$)$_2$PtCl$_6$ + 0.8 M Na$_2$HPO$_4$ at a current density of 5 mA cm^{-2} for 10 min, such that a smooth light grey deposit is obtained.

RESULTS AND DISCUSSION

Cu deposition

For calibration of the Pt/Au quartz crystal the electrodeposition of (bulk) Cu was chosen.

Cu was deposited onto Pt from 10^{-3} M CuSO$_4$ + 0.5 M H$_2$SO$_4$ at 0.06 V for a fixed time; thereafter, the deposit was dissolved during potential scan (20 mV s^{-1}) in a positive direction and the change in frequency with potential was recorded simultaneously with the voltammogram. The frequency change corresponding with the Cu dissolution was determined by taking the difference in frequency at 0.06 V with respect to that in Cu-free electrolyte, which is taken as the bare surface. From the voltammogram, the coulometric charge was obtained. Several runs were carried out with Cu deposits ranging from 3 to 14 mC. From these data the Sauerbrey constant was calculated with:

$$S = \frac{QMW}{\Delta fnFA},$$

Q = charge associated with Cu dissolution, MW = molecular weight of Cu, n = number of electrons, F = Faraday constant. This yields: $S = (17.6 \pm 2\%)$ ng Hz^{-1} cm^{-2}, in agreement with the theoretical value.
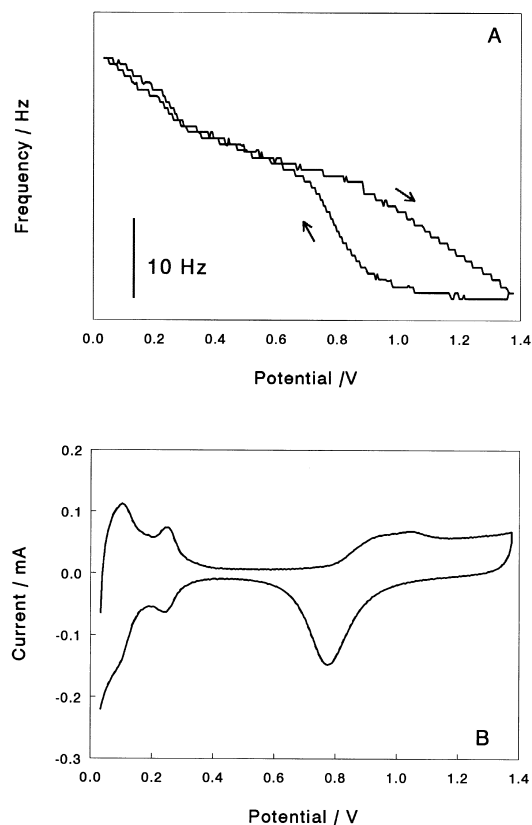

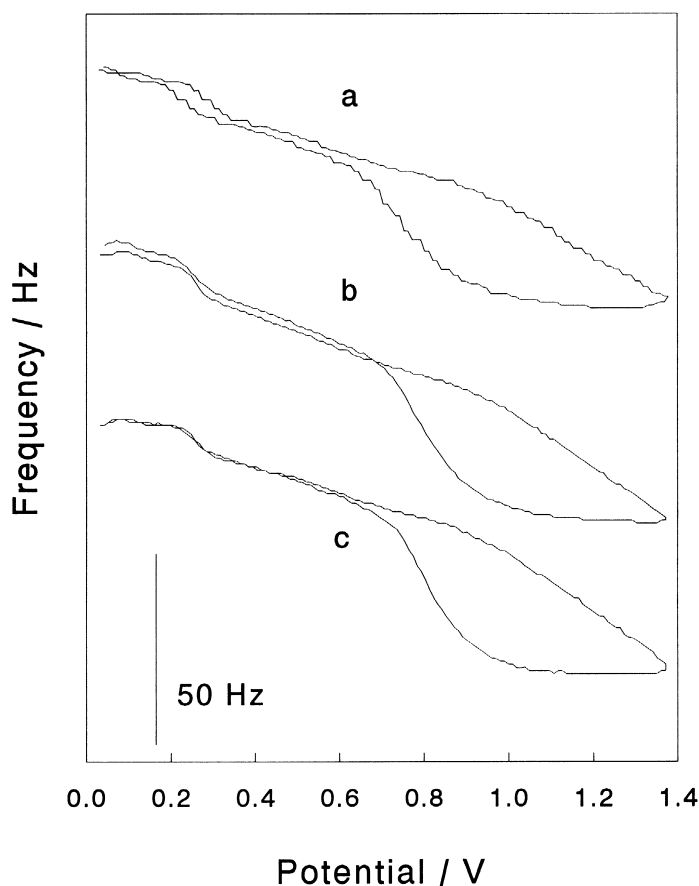Fig. 1. (A) Frequency–potential diagram and (B) voltammogram of Pt in 0.5 M H$_2$SO$_4$; scan rate 20 mV s^{-1}.

Fig. 2. Effect of scan rate on frequency–potential curve in 0.5 M H₂SO₄ for electrodeposited Pt (roughness factor 33). Scan rates: (a) 200, (b) 20 and (c) 5 mV s⁻¹.

Electrodeposited Pt; effect of roughness

Figure 1 gives the frequency–potential plot together with the voltammogram for Pt in 0.5 M H₂SO₄. Going from 0.03 to 1.4 V the frequency decreases and thus the mass increases over the whole potential range. The *f–E* curve shows a steep change in the H desorption area followed by a smaller change in the double layer region; in the hydrogen desorption area the frequency changes coincide with the H peak potentials. There is a further rapid frequency decrease concurrent with the start of the oxygen coverage. Changing the scan rate does not affect the frequency–potential pattern. The pattern of frequency change for the electrodeposited Pt is very similar to that observed on other types of Pt electrodes such as sputtered Pt [8, 9], film-coated Pt [10] or evaporated Pt [11]. The roughness factor of the electrodeposited Pt in Fig. 1 is 13 (calculated from Q_H with 0.21 mC cm⁻² for a Pt—H monolayer); the roughness factor of the film coated Pt is 3.5, for the evaporated Pt 13 and for the sputtered electrodes we calculated roughness factors 2–5. If a rougher deposit is applied (roughness factor 33), the *f–E* plot at the same scan rate [Fig. 2(b)] shows a different behaviour in the H desorption/adsorption range: the frequency

remains virtually constant up to 0.25 V and then decreases; furthermore, the frequency response in the low potential range varies with increasing scan rate, as shown by the other curves in Fig. 2. So electrodeposited Pt will only give the same mass balance results as smooth Pt if the roughness factor is low. Data obtained with rougher deposited Pt can be affected by the electrolyte present in the porous deposit, such an effect was also noted by Schumacher *et al.* [7].

Ageing can drastically alter the frequency response according to Raudonis *et al.* [16]. Using sputtered Pt (roughness factor 6–7) in 0.2 M H₂SO₄ they found a frequency decrease (mass increase) over the whole potential range of H desorption and O adsorption if the electrode is fresh and stabilized, but a frequency increase for a strongly aged electrode (more than 10,000 cycles). A less aged electrode (1000 cycles) shows an intermediate pattern of both an increase and a decrease of frequency. In their opinion such change in behaviour is not evoked by changes in roughness, although the voltammograms change in time. A similar frequency increase for Pt over the whole potential range was reported earlier [17], but it is not clear whether this concerns an aged electrode.

Wilde and Zhang [12, 13] also have used electro-deposited Pt on Au (roughness factor 20–30), but they found that the mass changes in the low potential region in 0.1 M HClO$_4$ differ with the scan rate; repeated cycling affected the results which were attributed to changes in area and structure.

Mass–potential behaviour in H$_2$SO$_4$ electrolyte

The frequency change of Pt during potential cycling was investigated in 0.1, 0.5 and 1 M H$_2$SO$_4$. All curves show a similar behaviour. The mass change per mol Pt can be calculated from the frequency change in the potential range of H desorption, taking into account the real surface area, given by Q_H. The results for the mass change in the H desorption area are summarized in Table 1; the values do not vary significantly with acid concentration. The literature data, also listed in this table, show some variation, but it is noted that the results are obtained by different authors.

The frequency change in the potential range corresponding with oxygen coverage was measured for potential scans to different end potentials up to 1.6 V. The oxide coverage at each end potential, $Q_O(E)$, was determined from the simultaneously recorded voltammograms. The total frequency change, determined with respect to the frequency at the initial potential (0.03 V), is plotted in Fig. 3 for 0.5 M H$_2$SO$_4$ as a function of the oxide coverage which is expressed as $Q_O(E)/2Q_H$ to exclude the roughness factor. The frequency varies linearly with oxygen coverage. The frequency data for the three sulfuric acid concentrations are converted to mass change per mol Pt, taking into account the Q_H value for each series; these results are given in Fig. 4. The slope of the curves increases with acid concentration. At $Q_O(E)/2Q_H = 0$ all curves reach virtually the same mass value, *ca* 9 g (mol Pt)$^{-1}$; this implies that the total mass change in the region of H desorption and double layer region does not vary with acid concentration. This is an interesting result, particularly in view of the fact that it has been established [18–24] that sulfate species adsorb on Pt in the range from *ca* 0.1 to 1.1 V, reaching a maximum around 0.6–0.8 V, with increasing concentration more sulfate
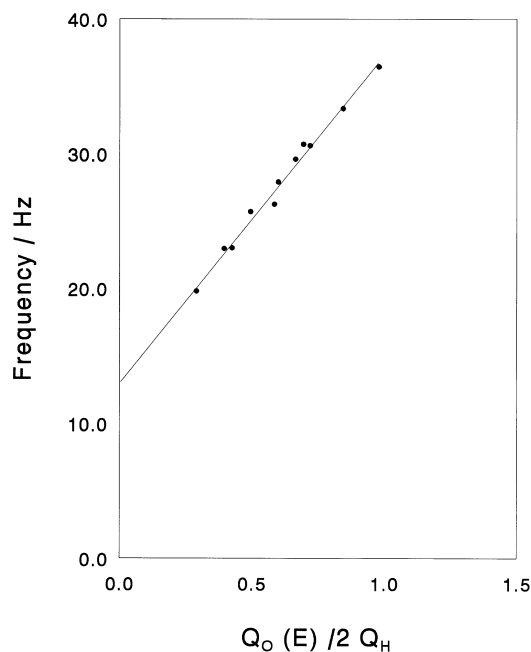
is adsorbed. At higher potentials (> 1 V) sulfate ions are included in the oxide layer. Shimazu and Kita [10] attribute the mass change in both H desorption and double layer region to water adsorption, whereas Watanabe *et al.* [8] argue that in the double layer region specific adsorption or coadsorption of bisulfate species takes place. Markovic *et al.* [23]

Fig. 3. Total frequency change vs oxide coverage $Q_O/2Q_H$ in 0.5 M H$_2$SO$_4$.

Table 1.
Mass change [g (mol Pt)$^{-1}$] in H desorption range in H$_2$SO$_4$

Concentration (M)	This work	Literature values	Reference
0.05		6.5[a]	8
0.1	6.3	5	9
		6.5	10
0.5	7.1	9	11
1	6.6		

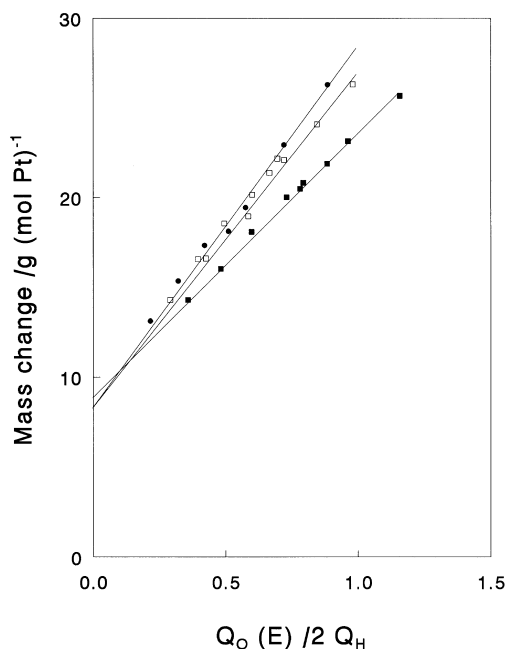[a]Estimated from their results.

Fig. 4. Total mass change vs oxide coverage $Q_O/2Q_H$; ■: 0.1, □: 0.5 and ●: 1 M H$_2$SO$_4$.

Table 2.
Mass change [g (mol Pt)$^{-1}$] for oxygen monolayer [$Q_O(E)/2Q_H = 1$] in H_2SO_4

Concentration (M)	This work	Literature values	Reference
0.05		17.2[a]	8
0.1	14.7	16	9
		17.9[b]	10
0.5	18.2	18.1[b]	11
1	19.9		

[a] Estimated from their results.
[b] Extrapolated from their results.

concluded from cyclic voltammetry data in the low potential range that sulfate anions are adsorbed only in the potential range corresponding with strongly adsorbed hydrogen, not as potentials of weakly adsorbed hydrogen.

So at this point we conclude that the observed mass change of *ca* 9 g (mol Pt)$^{-1}$ for hydrogen desorption and double layer region is due to adsorbed water and maybe some sulfate species. Whether indeed sulfate species are adsorbed in this potential region will be discussed in the next section, where the effect of different anions is investigated.

The mass value corresponding with a monolayer of oxygen can be obtained from Fig. 4 as the difference between the g mol^{-1} values at $Q_O(E)/2Q_H = 1$ and 0; this is given in Table 2. Literature data of mass balance experiments for oxygen coverage have been reported for one oxidation potential, therefore, these values were converted to monolayer coverage in order to compare the various results; these are also presented in Table 2.

The mass values for an oxygen monolayer are all close to 16 g (mol Pt)$^{-1}$. Earlier mass balance studies [9, 11] have concluded that this points to PtO. With *in situ* Raman spectroscopy of the oxidized layer, the presence of PtO has been reported [25]. It must be realized, however, that the results actually refer to a mass difference; so the mass change for a true PtO monolayer can only be obtained if the surface is bare at the potential where the oxide coverage begins. It is obvious from the results in Fig. 4 that this is certainly not the case. At the beginning of oxygen coverage there is already a mass increase of *ca* 9 g (mol Pt)$^{-1}$ compared with the state at 0.03 V. Another approach is therefore to consider the total difference in mass between the surface covered with an oxygen monolayer and the initial state at 0.03 V. The question then is whether the reference state at 0.03 V is adequately represented by a hydrogen monolayer (PtH). IR spectroscopy studies on adsorbed hydrogen have proved the presence of water [26, 27]. Bewick and Russell [26] suggest a model for a particular water structure on adsorbed hydrogen in which dimers of water molecules are present on the

weakly bonded hydrogen. On strongly bonded hydrogen this water structure is no longer observed. If we take their model, in which for each pair of water molecules three H sites are involved, we have for the coverage at 0.03 V: $(2 \times 18)/3 + 1 = 13$ g (mol Pt)$^{-1}$.

The total mass difference between oxygen monolayer and hydrogen monolayer then amounts to $16 - 13 = 3$ g (mol Pt)$^{-1}$ if the oxygen coverage consists of PtO and to $34 - 13 = 21$ g (mol Pt)$^{-1}$ for coverage with Pt(OH)$_2$. The experimental total mass difference data are higher than these values; they increase from 24 g (mol Pt)$^{-1}$ in 0.1 M H_2SO_4 to 28.5 g (mol Pt)$^{-1}$ in 1 M. Hence, it follows that at the potential where $Q_O(E)/2Q_H = 1$ the surface is not only covered with an oxygen monolayer, but also with coadsorbed H_2O and/or sulfate species, which increase with higher acid concentration. For example, if in 1 M acid a $H_2O \cdot SO_4$ species were present on top of a PtO layer, this would amount to a content of *ca* 22%. Whether the oxide species is PtO or Pt(OH)$_2$ cannot be concluded from these data.

The anion effect on the mass–potential behaviour

The frequency changes with potential were also measured in 0.5 M $HClO_4$ and in 0.5 M H_3PO_4 to investigate the role of the anion. The results obtained in 0.5 M $HClO_4$ are shown in Fig. 5. The mass change in the H region is about half of that in sulfuric acid, cf. Table 3. Our results agree with those of Shimazu and Kita [10]. Others [12–14] however report both a mass increase and decrease in 0.1 M $HClO_4$ in the low potential region. Hachkar *et al.* [14] found a mass decrease of 7 ng cm^{-2} (i.e. 3.2 g (mol Pt)$^{-1}$) during adsorption of strongly adsorbed H, but a mass increase of 11 ng cm^{-2} (i.e. 5.0 g (mol Pt)$^{-1}$) for weakly adsorbed hydrogen. Hence, over the whole potential range of H desorption a total mass decrease is obtained.

The frequency change in the oxide region was determined for different end potentials and the results of the total mass change with oxygen coverage are presented in Fig. 6. It is seen that the mass change until the beginning of oxygen coverage is 4.7 g (mol Pt)$^{-1}$, which accounts for H desorption and double layer region. This is much less than in the case of sulfuric acid. So we can therefore now conclude that in sulfuric acid both water and sulfate species (*ca* 4%) are adsorbed, whereas in perchloric acid only water is adsorbed in the low potential range. With IR spectroscopy the presence of hydronium in the H region was observed [28]. If we assume for the reference state at 0.03 V the same water adsorption structure as in sulfuric acid, it follows that at the beginning of oxygen coverage the surface is covered with a layer corresponding with 16.7 (= 12 + 4.7) g (mol Pt)$^{-1}$ or about a full monolayer of water. The mass change in the oxide region is lower in $HClO_4$ than in H_2SO_4.

The total mass change at $Q_O(E)/2Q_H = 1$ amounts to 18.9 g (mol Pt)$^{-1}$, indicating inclusion of H_2O
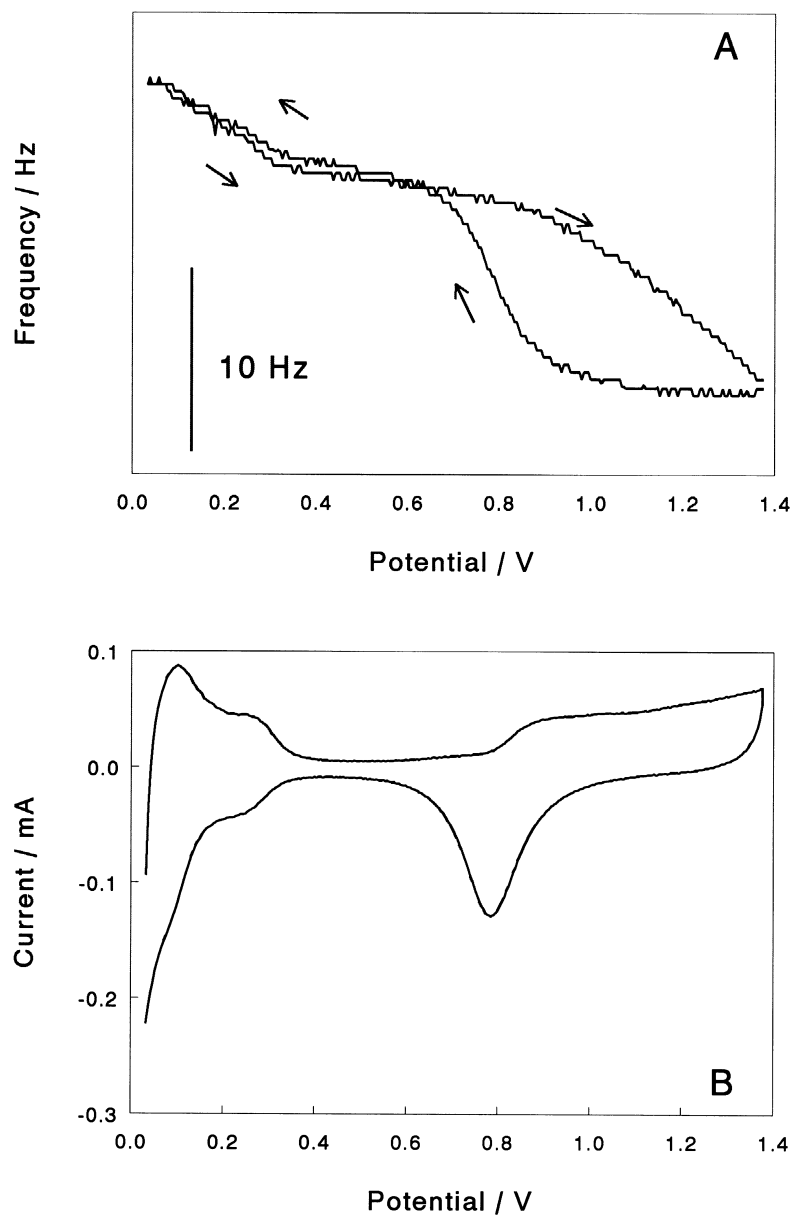
Fig. 5. (A) Frequency–potential diagram and (B) voltammogram of Pt in 0.5 M HClO$_4$; scan rate 20 mV s^{-1}.

and/or perchlorate on the oxygen layer. These findings are in agreement with IRAS measurements on Pt(111) [29], which showed that specific adsorp-

tion of perchlorate begins at 0.5 V and increases with potential to a maximum at 0.8 V.

The *f–E* curve in 0.5 M H$_3$PO$_4$ shows the same

Table 3.
Mass change [g (mol Pt)$^{-1}$] in HClO$_4$

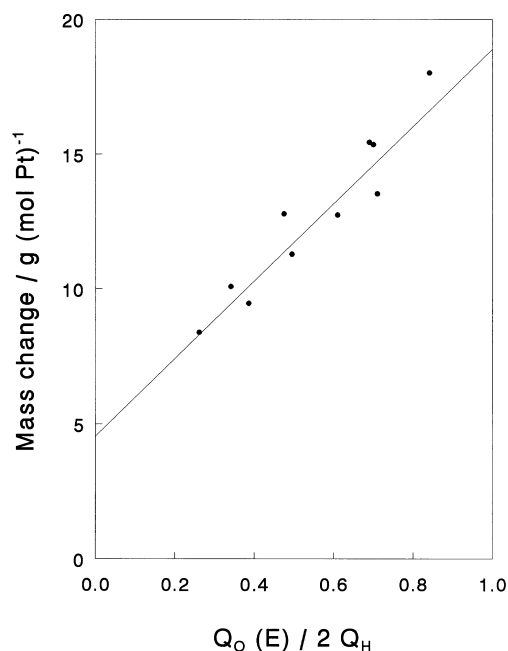|	Concentration (M)	This work	Literature values	Reference
H desorption	0.1		4.3	10
	0.5	3.9		
$Q_O(E)/2Q_H = 1$	0.1		13.8[a]	10
	0.5	14.2		

[a]Extrapolated from their results.

Fig. 6. Total mass change vs oxide coverage $Q_O/2Q_H$ in 0.5 M $HClO_4$.

patterm as in sulfuric acid. The mass change in H desorption region is larger than in 0.5 M H_2SO_4 so more phosphate is adsorbed than sulfate. The mass change for an oxygen monolayer is about the same in both electrolytes, see Table 4, which implies that water and phosphate are included in the oxide layer.

The anion effect was further investigated by carrying out measurements in 0.5 M p-toluene sulfonic acid, which introduces a heavier and larger anion (Fig. 7). As shown in Fig. 7(A) the frequency decreases during a positive potential scan in the H and O region only; there is virtually no change in the double layer range. The f–E curve resembles that of $HClO_4$; the total frequency change is about the same. Q_H is ca 50% of the value in perchloric acid, hence only half of the Pt molecules on the surface is available for H coverage in the presence of p-toluene sulfonic acid. From the frequency change in hydrogen desorption range a mass change of 4.5 g (mol Pt)$^{-1}$ is calculated (this refers to the available sites), which is about the same value as in perchloric acid; thus confirming the above conclusion that in perchloric acid only water molecules are adsorbed in

the low potential range. The sulfonic anion apparently does not desorb from the surface with increasing potential. The onset of oxide growth is strongly retarded in toluene sulfonic acid. The total mass change calculated from 0.03 to 1.4 V amounts to 24.4 g (mol Pt)$^{-1}$, at this potential the oxygen coverage $Q_O(E)/2Q_H = 1.1$. This mass value is higher than in perchloric acid and points to the presence of organic species on the sites not covered with p-toluene sulfonic acid from the beginning.

Mass–potential behaviour on 0.5 M KOH

All of the acid electrolytes show a mass increase with increasing potential. This has also been observed on Au [30]; however, in alkaline electrolyte a mass decrease over the H desorption and double layer region was reported on Au [4, 6]. This was attributed to cation desorption [4], although others [6] have interpreted these results as a change in the viscosity of the outer Helmholtz layer.

It was therefore decided to carry out a mass experiment on Pt in 0.5 M KOH. The frequency–potential curve (Fig. 8) shows initially a small variation, followed by a steep decrease in the oxide region. A similar behaviour was found in 0.1 M NaOH [10]. A slight maximum can be noted around 0.15 V; the total frequency decrease in the potential range between 0.45 and 1.1 V amounts to a mass increase of 15.9 g (mol Pt)$^{-1}$; the oxygen coverage reaches a value of $Q_O(E)/2Q_H = 0.69$, corresponding with 11.9 g (mol Pt)$^{-1}$. The frequency changes in the lower potential range amount to a few g (mol Pt)$^{-1}$, but are too small for a further evaluation. The fact

Table 4.
Mass changes [g (mol Pt)$^{-1}$] in 0.5 M H_3PO_4 and p-toluene sulfonic acid

Electrolyte	H desorption	$Q_O(E)/2Q_H = 1$
0.5 M H_3PO_4	8.4	16.5
0.5 M $CH_3C_6H_4SO_3H$	4.5	18.1
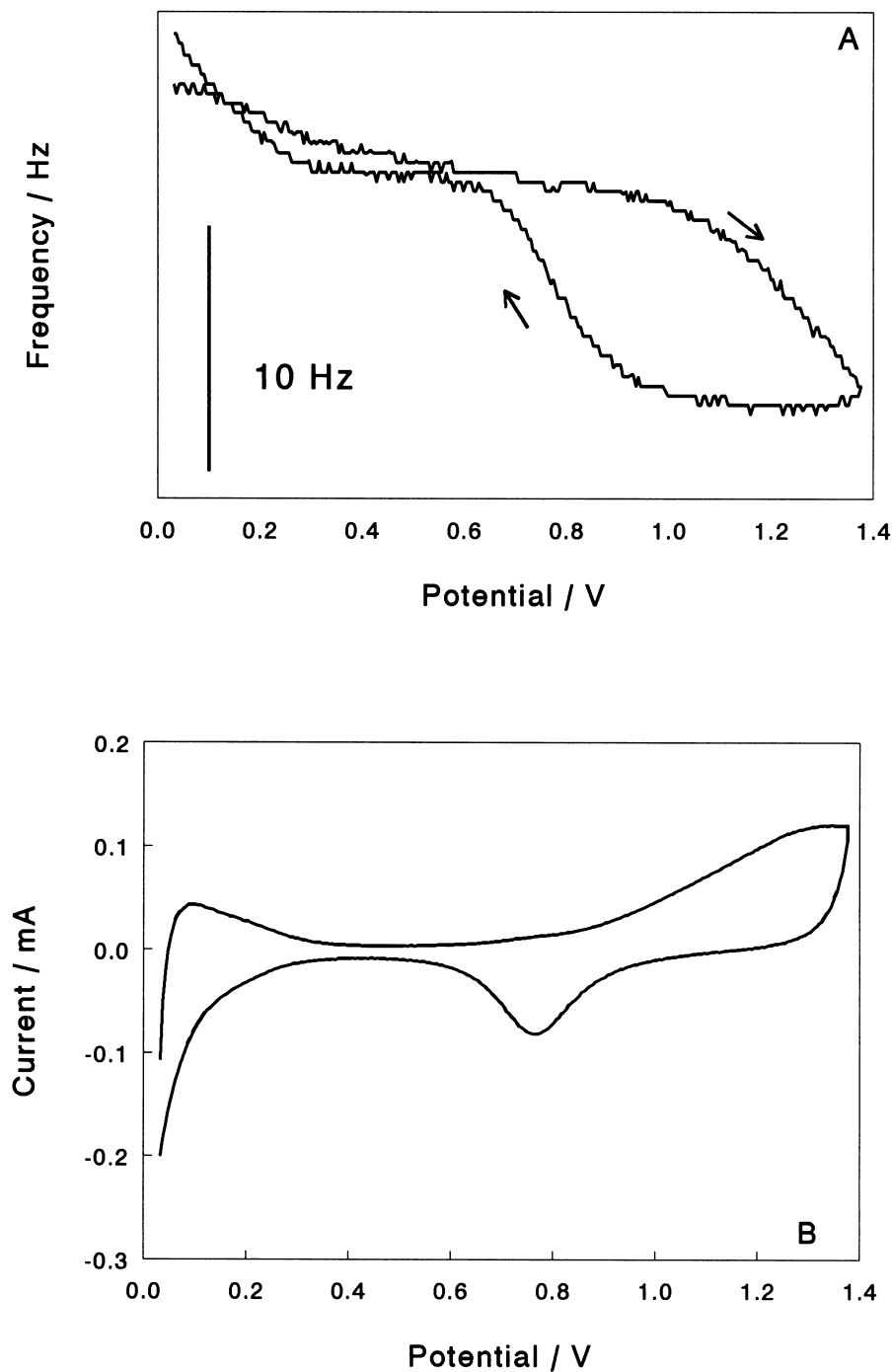
Fig. 7. (A) Frequency–potential diagram and (B) voltammogram of Pt in 0.5 M CH$_3$C$_6$H$_4$SO$_3$H (toluene sulfonic acid); scan rate 20 mV s^{-1}.

that these values are much smaller than in acid media indicates that in alkaline electrolyte, water molecules are not attached to the surface, due to the abundant presence of hydroxyl ions.

The frequency pattern at Pt does not show such a large difference between acid and alkaline electrolyte as is observed on Au. Hence, it is more likely that the changes on Au are due to difference in adsorption

than to change in viscosity of the adjacent layer. The mass decrease would thus imply a decrease in K$^+$ adsorption with increasing potential, accompanying the H desorption.

Mass changes due to CO adsorption and oxidation

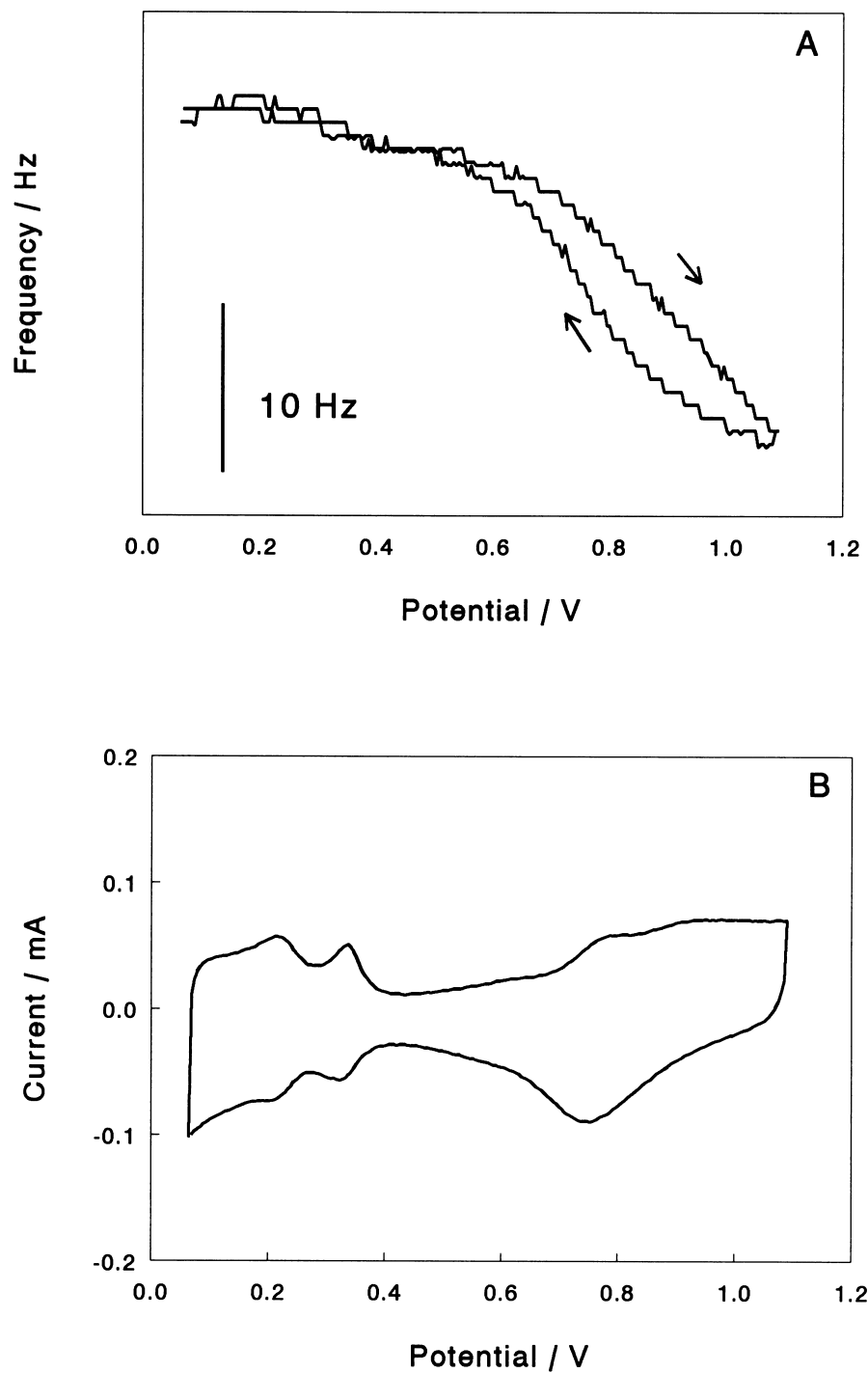On polycrystalline Pt at least two types of CO adsorbates can be formed depending on the

Fig. 8. (A) Frequency–potential diagram and (B) voltammogram of Pt in 0.5 M KOH; scan rate 20 mV s^{-1}.

adsorption conditions and the substrate structure [31–35]; the bridge bonded species is oxidized at lower potential than the linearly bonded CO which is the dominant species.

The electro-oxidation of CO adsorbate was studied for different adsorption potentials in 0.5 M H_2SO_4, 0.5 M $HClO_4$ and 0.5 M H_3PO_4. The experiments were carried out as follows: first a voltammogram and frequency plot were recorded in O_2-free electrolyte; then CO was introduced using a dilute (10%) CO–argon gas mixture, while the potential was kept at the adsorption potential for 5 min; thereafter the electrolyte was flushed with argon for 10 min while keeping the potential constant; after 10 min waiting period at that potential, the potential cycling was started in a negative direction. Figure 9(A) gives the voltammogram for CO adsorbate ($E_{ads} = 0.44$ V) in 0.5 M H_2SO_4 with an oxidation peak at 0.70 V. The corresponding frequency–potential curve [Fig. 9(B)] shows during the first positive going scan a gradual increase of frequency; beyond 0.7 V the frequency decreases. This occurs before the current maximum of the CO oxidation peak is reached. During the negative going scan the frequency increases to a final value that is higher than at the start, which demonstrates that adsorbed CO was measured indeed during the first scan. The frequency behaviour in the oxide region is identical to that in the CO-free electrolyte, the oxide growth is thus not affected by the presence of CO. At lower CO adsorption potential a prewave occurs in the voltammogram. Fig. 10(A) gives the result for CO adsorbed at 0.27 V. The presence of a more easily oxidizable CO adsorbate is indeed known to be found if CO is adsorbed at H_{ads} covered surface [36]. At the potential of the onset of the prewave the frequency [Fig. 10(B)] shows a more rapid increase; however, here again the decrease in frequency occurs at lower potential than the peak maximum. In ellipsometric measurements [15] we found also a significant change of the optical parameter Δ in the presence of CO adsorbate, but the adsorbate oxidation peak here coincides with a distinct change in Δ. It is remarkable that in the mass-balance measurements the main peak of the CO oxidation do not coincide with a distinct change in the frequency; moreover, already some mass decrease occurs before the CO oxidation starts. Apparently a non-electrochemical active species, most likely water, is desorbed in the low potential range, in contrast with a CO-free surface where the mass increases with potential. This corroborates the fact that enhanced water adsorption was found in the presence of CO with electrochemical thermal desorption mass spectrometry [37]; this means that water is adsorbed on top of CO_{ads}. The formation of a carbon monoxide hydrate was proposed earlier by Stonehart [38]. These water molecules are present on top of CO as dipoles with the positive pole towards CO. Hence, with increasing potential the positive charge increases and the water molecules (on top of CO) are being repulsed. If we assume that the part of the surface that is not covered with CO_{ads} behaves like the CO-free system, then with increasing potential water and anions should become adsorbed on these sites. However, Fig. 9(B) shows that in the positive scan the frequency at *ca* 0.7 V, *ie* before the CO oxidation, is even higher than in the negative going scan where CO has been oxidized. This means that the presence of CO hinders adsorption of water and/or anions on the sites not covered by CO.

The mass change associated with adsorbed CO is obtained from the difference in frequency in the presence and absence of CO_{ads} at 0.03 V. The CO coverage is obtained from the anodic peak in the corresponding voltammogram with $\theta = Q_{CO}/2Q_H$; Q_H is taken from the blank experiment. The data are presented in Table 5 together with the mass values calculated from the coulometric coverage for 1 CO per Pt [= 28 g (mol Pt)$^{-1}$]. Although it is argued above that the measured amount comprises both adsorbed CO and water, the values are much lower than the value predicted by the coulometric data.

It was discussed earlier that the reference state of Pt contains adsorbed water on top of the hydrogen monolayer and it was assumed that this corresponds with 13 g (mol Pt)$^{-1}$. The amount of water adsorbed on CO (Δm_w) can be determined from the frequency differences at 0.7 and 0.03 V, although we do not know whether this value represents all of the adsorbed water on top of CO_{ads}. We can now make a tentative calculation of the total mass change due to CO coverage with respect to the CO-free surface:

$$\Delta m_{calc} = \{\theta_{CO} \times 28 + \Delta m_w + (1 - \theta_{CO}) \times 13\} - 13.$$

For $E_{ads} = 0.44$ V with $\Delta m_w = 3.0$ g (mol Pt)$^{-1}$ this yields $\Delta m_{calc} = 11.1$ g (mol Pt)$^{-1}$; for $E_{ads} = 0.27$ V and $\Delta m_w = 4.7$ g (mol Pt)$^{-1}$ this yields $\Delta m_{calc} = 14.3$ g (mol Pt)$^{-1}$. These values are close to the experimental mass values. It could imply that indeed all the water on CO was measured in the frequency increase; moreover, it can be considered as a confirmation of the assumed model for the water structure in the reference state.

The electrooxidation of CO_{ads} in 0.5 M $HClO_4$ gives similar results as in sulfuric acid; Fig. 11 displays the i/E and f/E curves for $E_{ads} = 0.43$ V. From the initial frequency increase at low potential it follows that also in perchloric acid water is adsorbed on CO. The CO mass change data are summarized in Table 6 and show a similar large discrepancy between the coulometric and mass values as in sulfuric acid. If the same reference state may be taken as in the case of sulfuric acid, $\Delta m_{calc} = 12.8$ g (mol Pt)$^{-1}$ for $E_{ads} = 0.43$ V with $\Delta m_w = 4.1$ g (mol Pt)$^{-1}$; for $E_{ads} = 0.32$ V and $\Delta m_w = 4.4$ g (mol Pt)$^{-1}$ $\Delta m_{calc} = 13.8$ g (mol Pt)$^{-1}$. There remains a discrepancy, which might imply that the assumption about the reference state was not correct. Measurements of Hachkar *et al.* [14] in CO saturated 0.1 M $HClO_4$ also show some mass decrease before the
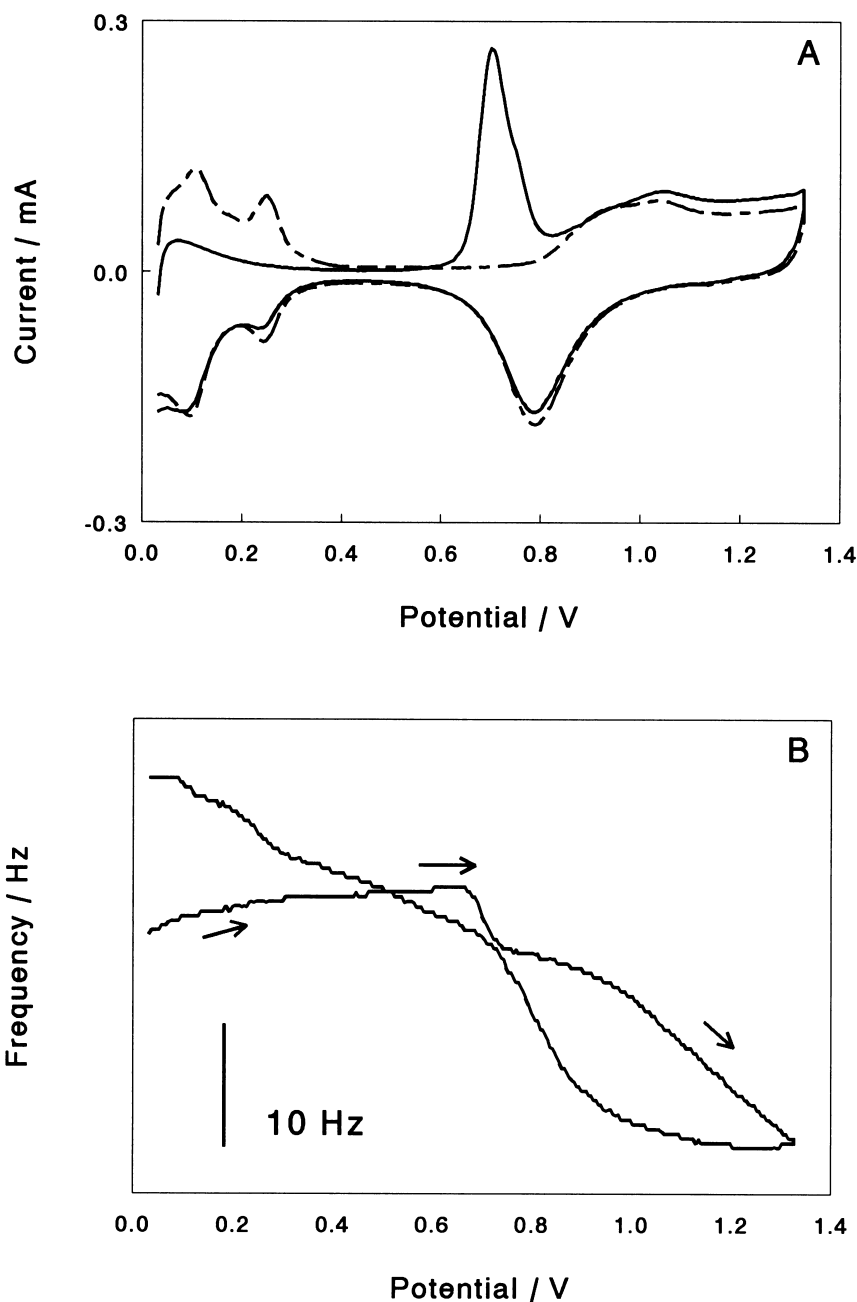
Fig. 9. (A) Voltammogram and (B) frequency–potential diagram in the presence of adsorbed CO in 0.5 M H_2SO_4; dashed line: blank electrolyte; E_{ads} = 0.44 V; scan rate 20 mV s^{-1}.

actual CO oxidation starts; the total mass decrease amounts to *ca* 25 ng cm^{-2} [11.5 g (mol Pt)$^{-1}$] for an (assumed) full coverage with CO, which is comparable to the results reported here.

The results for the oxidation of the CO adsorbate in 0.5 M H_3PO_4 (Fig. 12) differ from those in sulfuric and perchloric acid. The voltammogram (E_{ads} = 0.37 V) shows a much broader CO oxidation peak
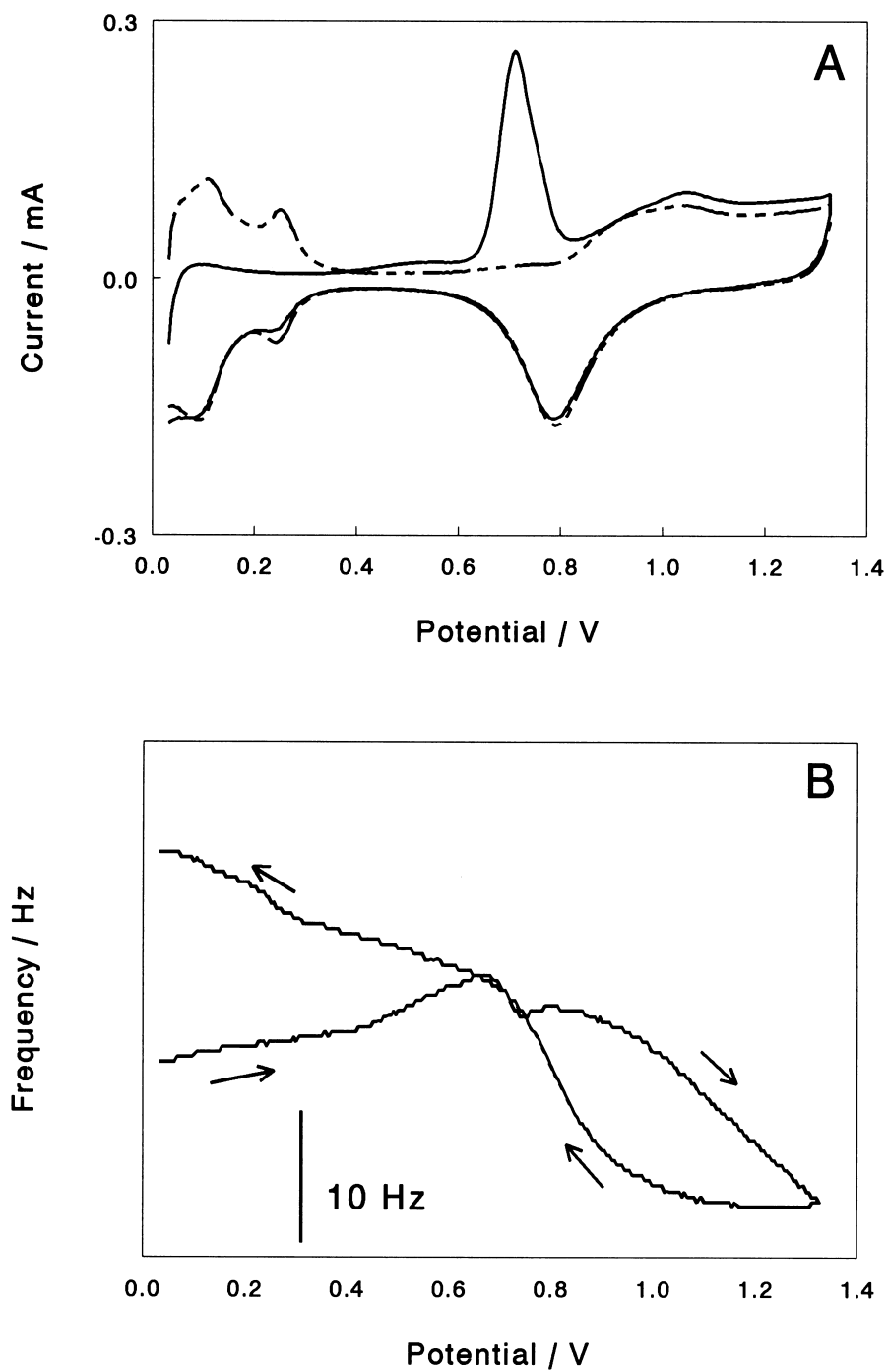
Fig. 10. (A) Voltammogram and (B) frequency–potential diagram in the presence of adsorbed CO in 0.5 M H_2SO_4; dashed line: blank electrolyte; $E_{ads} = 0.27$ V; scan rate 20 mV s^{-1}.

Table 5.
Mass change for CO_{ads} in 0.5 M H_2SO_4

E_{ads} (V)	θ_{CO}	g (mol Pt)$^{-1}$ calc. from θ_{CO}	g (mol Pt)$^{-1}$ Δf measurement
0.44	0.54	15.1	10.7
0.37	0.60	16.8	10.7
0.32	0.64	17.9	10.8
0.27	0.64	17.9	12.4

Table 6.
Mass change for CO_{ads} in 0.5 M $HClO_4$

E_{ads} (V)	θ_{CO}	g (mol Pt)$^{-1}$ calc. from θ_{CO}	g (mol Pt)$^{-1}$ Δf measurement
0.43	0.58	16.2	8.6
0.37	0.62	17.4	8.3
0.33	0.63	17.6	10.8
0.27	0.64	17.9	12.4

around 0.8 V and the frequency change now coincides with the coulometric change. Moreover, the mass changes for CO adsorbate, listed in Table 7, are far better in agreement with the coulometric data. An explanation could be that the reference state of Pt is different from that in sulfuric acid in the sense that in the case of phosphoric acid no water is adsorbed on the hydrogen monolayer or on Pt. Whether there
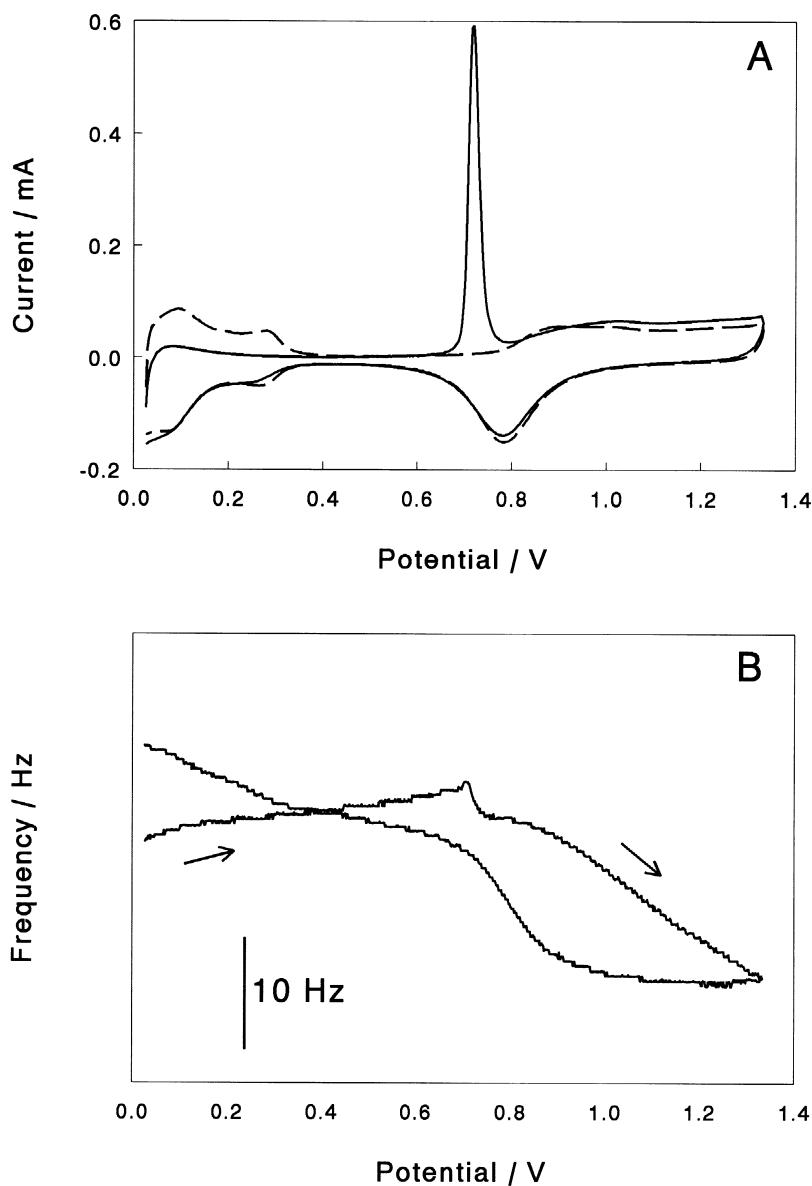

Fig. 11. (A) Voltammogram and (B) frequency–potential diagram in the presence of adsorbed CO in 0.5 M $HClO_4$; dashed line: blank electrolyte; $E_{ads} = 0.43$ V; scan rate 20 mV s^{-1}.
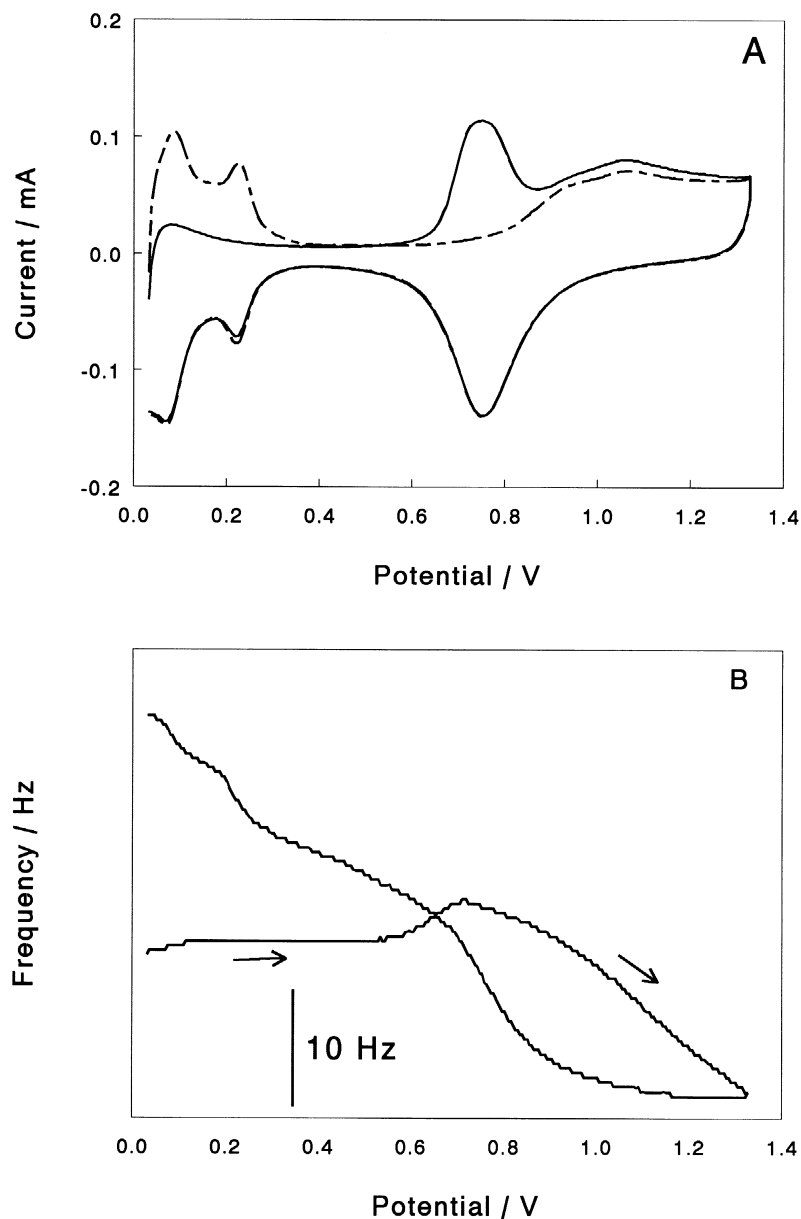
Fig. 12. (A) Voltammogram and (B) frequency–potential diagram in the presence of adsorbed CO in 0.5 M H_3PO_4; dashed line: blank electrolyte; $E = 0.37$ V; scan rate 20 mV s^{-1}.

also some anion adsorption on top of CO plays a role is difficult to ascertain.

The effect of the CO adsorption potential is much less in phosphoric acid than in sulfuric or perchloric acid; no prewave is observed at lower adsorption potential, At low potentials there is an initial frequency increase, but this is much smaller. A possible explanation for the difference in mass change around the CO peak in the three electrolytes could be that the oxidation of the CO adsorbate in sulfuric and perchloric acid occurs so fast (over a small potential range) that after the disappearance of CO the free sites are immediately covered with water molecules, whereafter the surface oxidation begins. In phos-

phoric acid more different sites are involved, the oxidation of the CO adsorbate occurs over a broader potential range.

Table 7.
Mass change for CO_{ads} in 0.5 M H_3PO_4

E_{ads} (V)	θ_{CO}	g (mol Pt)$^{-1}$ calc. from θ_{CO}	g (mol Pt)$^{-1}$ Δf measurement
0.42	0.45	12.6	15.7
0.37	0.47	13.2	15.2
0.32	0.51	14.3	16.7
0.27	0.47	13.2	15.8

CONCLUSIONS

The mass change of Pt was investigated during potential scanning in acid electrolytes. In the oxygen region the mass increases linearly with increasing oxygen coverage. The mass change is larger with higher sulfuric acid concentration, implying incorporation of sulfate species in the oxide layer. The total mass change in the potential range up to the beginning of the oxygen coverage, however, does not vary with sulfuric acid concentration.

The total mass change in the H desorption range depends on the type of electrolyte anion: Δm (H_3PO_4) > Δm (H_2SO_4) > Δm ($HClO_4$). It is concluded that in the low potential range the surface becomes increasingly covered only with water molecules in the case of perchloric acid, while in the case of sulfuric and phosphoric acid also some sulfate respectively phosphate species are included.

The mass balance measurements of the Pt/CO_{ads} system in sulfuric acid, perchloric acid and phosphoric acid show a mass increase compared with the CO-free electrolyte. On top of the adsorbed CO water is present, which disapears with increasing potential before CO is oxidized.

Moreover, it follows from the difference between the frequency–potential curves in the presence and absence of CO_{ads} that the reference state of Pt at 0.03 V is not the same in the different electrolytes. It is concluded that water molecules are attached to adsorbed hydrogen at 0.03 V in H_2SO_4 and $HClO_4$, but not in H_3PO_4. So, in spite of Horanyi's warning [5] that detection of water is questionable, we think that the presence of adsorbed water can be deduced from our mass-balance measurements. On the other hand, it must be realized that the EQCM technique gives information on the mass changes occurring at the electrode/electrolyte interface during potential scanning, but does not reveal which species is involved. This must be concluded from calculated models for the different possible adsorbates. It is therefore recognized that the conclusions presented here are somewhat hypothetical and are subject to further confirmation by *in situ* spectroscopic methods.

REFERENCES

1. D. A. Buttry, in *Electroanalytical Chemistry* (Edited by A. J. Bard) Vol. 17, p. 1. Marcel Dekker, New York (1991).
2. D. A. Buttry and M. Ward, *Chem. Rev.* **92,** 1355 (1992).
3. C. Lu (Editor), *Applications of Piezoelectric Quartz Crystal Microbalances*, Vol. 7. Elsevier, Amsterdam (1984).
4. W. Kautek, M. Sahre and D. M. Soares, *Ber. Bunsenges. Phys. Chem.* **99,** 667 (1995).
5. G. Horanyi, Specialist Periodical Report, *Catalysis*, **12,** 255 (1996).
6. V. Tsionsky, L. Daikhin and E. Gileadi, *J. Electrochem. Soc.* **142,** L233 (1995).
7. R. Schumacher, J. G. Gordon and O. Melroy, *J. Electroanal. Chem.* **216,** 127 (1987).
8. M. Watanabe, H. Uchida and N. Ikeda, *J. Electroanal. Chem.* **380,** 255 (1995).
9. V. I. Birss, M. Chang and J. Segal, *J. Electroanal. Chem.* **355,** 181 (1993).
10. K. Shimazu and H. Kita, *J. Electroanal. Chem.* **341,** 361 (1992).
11. T. Frelink, W. Visscher and J. A. R. van Veen, *Langmuir* **12,** 3702 (1996).
12. C. P. Wilde and M. Zhang, *J. Electroanal. Chem.* **327,** 307 (1992).
13. C. P. Wilde and M. Zhang, *J. Electroanal. Chem.* **340,** 241 (1992).
14. M. Hachkar, T. Napporn, J.-M. Leger, B. Beden and C. Lamy, *Electrochim. Acta* **41,** 2721 (1996).
15. T. Frelink, W. Visscher, A. P. Cox and J. A. R. van Veen, *Ber. Bunsenges. Phys. Chem.* **100,** 599 (1996).
16. R. Raudonis, D. Plausinaitis and V. Daujotis, *J. Electroanal. Chem.* **358,** 351 (1993).
17. W. Stöckel and R. Schumacher, *Ber. Bunsenges. Phys. Chem.* **91,** 345 (1987).
18. A. Wieckowski, P. Zelenay and K. Varga, *J. Chim. Phys.* **88,** 1247 (1991).
19. F. C. Nart and T. Iwasita, *J. Electroanal. Chem.* **308,** 277 (1991).
20. F. C. Nart, T. Iwasita and M. Weber, *Electrochim. Acta* **39,** 961 (1994).
21. K. Kunimatsu, M. G. Samant and H. Seki, *J. Electroanal. Chem.* **258,** 163 (1989).
22. K. Varga, P. Zelenay and A. Wieckowsky, *J. Electroanal. Chem.* **330,** 453 (1992).
23. N. M. Markovic, N. S. Marinkovic and R. R. Adzic, *J. Electroanal. Chem.* **241,** 309 (1988).
24. N. M. Markovic, N. S. Marinkovic and R. R. Adzic, *J. Electroanal. Chem.* **314,** 289 (1991).
25. T. Maeda, Y. Sasaki, C. Horie and M. Osawa, *J. Electron. Spectrosc. Related Phenomena* **64/65,** 381 (1993).
26. A. Bewick and J. W. Russell, *J. Electroanal. Chem.* **132,** 329 (1982).
27. K. Kunimatsu, M. G. Samant and H. Seki, *J. Electroanal. Chem.* **258,** 163 (1989).
28. J. B. Benziger, F. A. Pascal, S. L. Bernasek, M. P. Soriaga and A. T. Hubbard, *J. Electroanal. Chem.* **198,** 65 (1986).
29. Y. Shingaya and M. Ito, *J. Electroanal. Chem.* **372,** 283 (1994).
30. J. S. Gordon and D. C. Johnson, *J. Electroanal. Chem.* **365,** 267 (1994).
31. B. Beden, C. Lamy, N. R. de Tacconi and A. J. Arvia, *Electrochim. Acta* **35,** 691 (1990).
32. J. Sobkowsky and A. Czerwinski, *J. Phys. Chem.* **89,** 365 (1985).
33. K. Kunimatsu, W. G. Golden, H. Seki and M. R. Philpott, *Langmuir* **1,** 245 (1985).
34. K. Kunimatsu, H. Seki, W. G. Golden, J. G. Gordon II and M. R. Philpott, *Langmuir* **2,** 464 (1986).
35. A. Wieckowsky, M. Rubel and C. Gutiérrez, *J. Electroanal. Chem.* **382,** 97 (1995).
36. E. Santos, E. P. M. Leiva, W. Vielstich and U. Linke, *J. Electroanal. Chem.* **227,** 199 (1987).
37. E. El-Behaedi, H. W. Buschmann, T. Iwasita, W. Vielstich and M. M. Ghoneim, *Russ. J. Electrochem.* **31,** 1111 (1995).
38. P. Stonehart, *Electrochim. Acta* **18,** 63 (1973).